

https://dspace.org/

Interactions of alcohol and combination antiretroviral cART drug in diabetic male Sprague Dawley rats Hippocampal perturbations and toxicosis

Jaclyn Johnson; Robert Ndou; Ejikeme Mbajiorgu

https://hdl.handle.net/10539/42751
SCOPUS

Downloaded from a DSpace repository. https://dspace.org/

Toxicology Reports 10 (2023) 155–170

Contents lists available at ScienceDirect

Toxicology Reports

journal homepage: www.elsevier.com/locate/toxrep

Interactions of alcohol and combination antiretroviral (cART) drug in diabetic male Sprague Dawley rats: Hippocampal perturbations and toxicosis

Jaclyn Asouzu Johnson *, Robert Ndou, Ejikeme Felix Mbajiorgu

School of Anatomical Sciences, University of the Witwatersrand, Faculty of Health Sciences Johannesburg, South Africa

ARTICLE INFO

Handling Editor: Prof. L.H. Lash

Keywords:
Diabetes
Hippocampus
Neurogenesis
Antiretroviral
Alcohol
Histopathology
Toxicosis

ABSTRACT

Hippocampal pathology in diabetes is constantly investigated but the resultant health impact of the concomitant presence of alcohol and combined antiretroviral therapy (cART) in diabetes requires further studies to delineate toxicities inimical to hippocampal normal function. Forty-eight male Sprague Dawley rats were divided into eight groups (n = 6): negative control (NC), alcohol (AL), cART (AV), alcohol-cART (AA), diabetic control (DB), diabetes-alcohol (DAL), diabetes-cART (DAV), and diabetes-alcohol-cART (DAA) exposure groups. Following diabetes induction and sub-chronic (90 days) treatment exposure, hippocampal homogenates were profiled for pro-inflammatory cytokines and oxidative stress (MDA and GPx) using immunoassay, while apoptotic genes (BAX, Bcl_2, and Caspase-3), insulin receptor genes (INSR and IRS-1), and blood-brain barrier (BBB) junctional proteins (claudin-5, and occludin) gene expression were assessed using qPCR. Histomorphology of hippocampal neuronal number, nuclei area, and volume of dentate gyrus and neurogenesis were accessed using Giemsa stain, Ki67, and DCX histochemistry respectively. A central hippocampal effect that underpins all treatments is the reduction of DG neuronal number and antioxidant (GPx), highlighting the venerability of the hippocampal dentate gyrus neurons to diabetes, alcohol, cART, and their combinatorial interactions. Additionally, elevated BAX, Bcl_2, and IRS1 mRNA levels in the DAL group, and their downregulation in AA, suggests IRS-1-regulated apoptosis due to differential modulating effects of alcohol treatment in diabetes (DAL) in contrast to alcohol with cART (AA). Although the interaction in AA therapy ameliorated the independent alcohol and cART effects on MDA levels, pro-inflammatory cytokines, and DCX, the interaction in AA exacerbated a deficiency in the expression of INSR, IRS-1 (insulin sensitivity), and BBB mRNA which are implicated in the pathogenies of diabetes. Furthermore, the diabetic comorbidity groups (DAV, DAL, and DAA) all share a central effect of elevated hippocampal oxidative stress, BAX, and Caspase-3 mRNA expression with the reduced number of hippocampal neurons, dentate gyrus volume, and neurogenesis, highlighting neurodegenerative and cognitive deficiency implication of these comorbidity treatments. Considering these findings, assessment of hippocampal well-being in patients with these comorbidities/treatment combinations is invaluable and caution is advised particularly in alcohol use with cART prophylaxis in diabetes.

1. Introduction

Type 2 diabetes (T2D) is one of the most common chronic health and socio-economic problems in South Africa and globally [59,73]. Diabetes is classified into the general categories of type 1, type 2, gestational diabetes, and specific type of diabetes [6]. Specific diabetes includes monogenic diabetes syndrome, diseases of the exocrine pancreas, and recently drug or chemical-induced diabetes such as disease (for example Covid-19) associated diabetes [1]. Incidentally, combined antiretroviral therapy (cART), the first-line drug for the treatment of HIV/AIDS has been associated with metabolic syndrome and the pathogenesis of type 2 diabetes [12,45]. Additionally, lifestyle factors such as alcohol use/abuse can exert chemotoxicity, resulting in diabetes [14,25]. Consequently, chronic cART-induced diabetes is gradually becoming prevalent as a high proportion of individuals who are on chronic medications and regularly use alcohol may develop diabetes [23,36]. As reports indicate the continued spread of HIV/AIDS and cART in sub-Saharan Africa and globally [68,71], it is therefore of interest to

* Corresponding author.
E-mail addresses: jaclyn.johnson@wits.ac.za (J. Asouzu Johnson), robertndou@smu.ac.za (R. Ndou), ejikeme.mbajiorgu@wits.ac.za (E.F. Mbajiorgu).

https://doi.org/10.1016/j.toxrep.2023.01.009
Received 4 November 2022; Received in revised form 7 January 2023; Accepted 19 January 2023
Available online 20 January 2023
2214-7500/© 2023 The Authors. Published by Elsevier B.V. This is an open access article under the CC BY-NC-ND license (http://creativecommons.org/licenses/by-nc-nd/4.0/).

Please note that certain pages of this article have been removed in order to reduce the file size so that the PDF can be uploaded on the system (the system has a limit of 1MB for files and several PDF files are larger than this).

The first and last pages of each paper (with full bibliographic details and affiliations) are included.

If the entire unredacted paper is required, this can be emailed directly to whomever requires them by contacting Dr. Busisiwe Maseko on Busisiwe.Maseko@wits.ac.za

investigate the possible combined impact of cART and alcohol intake in diabetic individuals. Furthermore, this alcohol cART co-morbidity under a diabetic condition may require multiple drug therapy investigations to elucidate its health impact, especially on glucose-sensitive organs such as the brain.

The hippocampus is sensitive to insulin signalling and glucose homeostasis for the regulation of cognitive, memory, neurogenesis, and neuroprotective functions [34,53,70]. Hippocampal neurons and endothelial cells contain several membrane-bound insulin receptors (INSR), which recruit intracellular adapter proteins; insulin receptor substrate (IRS-1) in the canonical insulin signalling and mediate glucose uptake into cells [75]; [21]; [50]. Additionally, the penetration of drugs, chemicals, and inflammatory cytokines produced by microglial cells, into the hippocampus is tightly regulated [13,32] through junctional blood-brain barrier (BBB) proteins claudin-5 and occludin [19] located on hippocampal endothelial cells. However, the presence of chemical toxicants can disturb the BBB structural integrity. Therefore, the presence of alcohol, cART and diabetes may induce perturbations in the normal physiological regulation of insulin receptors, BBB proteins, and cytokines which may induce a cascade of events associated with oxidative stress, apoptosis, and compromised neurogenesis which are all independently reported in alcohol, cART, and diabetes [26,54,67,72]. Similarly, diabetes, alcohol, and cART are independently associated with hippocampal and cognitive impairment [44,46,58], and consequently their comorbidity (cART+ diabetes) showed an exacerbated effect [5]. However, the interaction of alcohol use with diabetes (alcohol +diabetes), the concomitant presence of cART and alcohol in the normal rat hippocampus (cART +alcohol), and in the diabetic hippocampus (alcohol + cART + diabetes) remains unclear. Therefore, the adverse effects of the co-presence of alcohol, cART, and diabetes on some molecular and histopathological parameters in the hippocampus that may negatively impact cognition require further elucidation for possible related neuropathological effects, especially as it relates to diabetic individuals living with HIV/AIDS, who consume alcohol regularly.

Clinical management of comorbidity patients often requires multiple drug therapy which commonly is associated with several independent side effects but cumulative drug-drug interaction between therapies [30, 39] could together become detrimental to overall patient health. Therefore, this study is designed to investigate the dual presence of cART administration and alcohol intake in type 2 diabetes for its attendant hippocampal effects relative to oxidative stress, neurogenesis and hippocampal insulin receptors. Additionally, we investigated the differential hippocampal toxicosis that may exists following the interaction of alcohol with cART, and the interactions of either alcohol or cART with diabetes in contrast to the hippocampal toxicity independently induced by alcohol, cART and diabetes.

Additionally, the use of an HIV naïve model in the current study excluded the possible impact (pathologies) associated with the presence of HIV on tissue-drug-disease interactions and enabled the toxicity of diabetes + alcohol + cART combinations to be studied and documented. We hypothesized that oxidative stress and neuroinflammation are central to most of the hippocampal pathologies induced. We used hippocampal tissue homogenates for the analysis of pro-inflammatory cytokines, oxidative and anti-oxidative enzymes. To evaluate the diabetogenic, metabolic, and neurodegenerative effects of these treatments specifically on the hippocampus, the molecular expression for insulin receptors and apoptosis in the hippocampus was described. We illustrate the histopathology of our molecular and biochemical findings by evaluating the impact of these treatments on the histomorphometry and immunostaining of neurons for associated toxicosis such as atrophy and deficit neurogenesis. We showed a novel effect of deficit antioxidant and dentate gyrus neurons as a uniform pathological effect across all different combinations of treatments.

2. Materials and methods

2.1. Chemicals

Oxidative stress markers were assessed using a malondialdehyde (MDA) Colorimetric assay kit: TBA method (Elabscience, Houston, Texas USA; E-BC-K025-M), and Glutathione Peroxidase (GSH-Px) Activity Assay Kit (Elabscience, Houston, Texas USA; E-BC-K096-M WST-1 Method). For PCR, TRIzol reagent (Merck; T9424), iso-propanol (Merck; B6916), cDNA using a high-capacity cDNA RT kit (Applied Biosystems; 4368814), Power Up SYBER Green Master Mix (Applied Biosystems; A25742; Austin, Texas, USA), Forward and Reverse Primer were procured from Inqaba Biotechnical industries (Hatfield, Pretoria, South Africa).

2.2. Animal housing

Forty-eight adult male Sprague Dawley rats were housed separately under clean conditions in cages. For the duration of the experiment, the rats had free access to drinking water or alcohol, and rat chow according to their allocated group treatment. Daily water or alcohol intake and weekly normal rat chow consumed in treated and untreated animals were measured by recording the amount of water or alcohol remaining using a measuring cylinder and weighing the remaining rat chow. The rats were weighed weekly, and non-fasting glucose tests, biweekly fasting glucose tests, and monthly oral glucose tolerance tests were carried out.

2.3. Experimental design

The rats were divided into eight groups (n = 6), the first four groups consist of non-diabetic animals and include; Negative control, untreated animals (NC), alcohol alone, received 10% alcohol in distilled water v/v ad libitum (AL), cART alone, received only antiretroviral medication 23.22 mg /Kg body weight daily as an extrapolated daily recommended cART dose (containing efavirenz 600 mg+ emtricitabine 200 mg+ tenofovir 245 mg) in gelatine cubes (AV), alcohol and cART, received the same dose of alcohol and cART (AA). The gelatine route of administration used in the present study was chosen to mimic the recommended oral route of administration of cART. The animals body weight was used to calculate the equivalent dose of cART which was added to gelatine pellets and daily fed to the animals orally. The other four groups consist of animals in which diabetes was induced using previously reported adapted protocol involving streptozotocin and fructose feeding [5,74]. These diabetic groups include, diabetic control, diabetic with no treatment (DB), diabetes and alcohol administration (DAL), diabetes and cART treatment (DAV), and diabetes, alcohol, and ART (DAA), all treatments commenced with the rats at 13 weeks of age-old and were carried out for 90 days after which animals were terminated, brains excised, and One hemisphere was fixed in 0.4 paraformaldehyde for histology and the other hemisphere was stored at − 80°C for immunoassay and molecular analysis.

2.4. Quantitative qPCR for junctional proteins, insulin receptors, and apoptotic markers

2.4.1. RNA extraction

From each brain sample, total RNA was extracted by homogenizing samples in TRIzol reagent (Merck; T9424) at a ratio of 30 mg tissue to 1000 μl Tri-reagent using a handheld tissue grinder G-50 (Coyote Bioscience, Jiangsu, China). The homogenates were vortexed for 15 s, followed by 200 μl of chloroform vortexed again and allowed to stand for 3 min at room temperature. The samples were centrifuged at 14,000 rpm for 15 min, the supernatant was collected, and 500 μl iso-propanol (Merck; B6916) was added and centrifuged at 14,000 rpm for 15 min. The supernatant was decanted and 1000 μl of 75% alcohol was added to

the pellet and centrifuged at 8000 rpm for 5 min. Alcohol was poured off and pellets were resuspended in RNAase-free water, heated at 60 °C, cooled then stored at − 80°C for further analysis. Subsequently, the RNA samples were analysed using a Nano-Drop® spectrophotometer, Series ND-100 to determine the RNA concentration and purity, thereafter RNA samples were stored at 80 °C.

2.4.2. cDNA synthesis

RNA samples were diluted according to their concentrations to a final concentration of 50 μg/μl. Total RNA was used in a reverse transcriptase reaction to synthesize cDNA using a high-capacity cDNA RT kit (Applied Biosystems; 4368814). Ten microlitres of 2x RT master mix and 10 μl of RNA samples were pipetted into each well of a 96-well plate, which were centrifuged at 2500 rpm for 2 min. The thermocycler for a reaction volume of 20 μl was set at 25 °C for 10 min, 37 °C for 60 min x2, 85 °C for 1 min, and 4 °C for infinity.

2.4.3. qPCR experiment

The standard guidelines and minimum information for publication of quantitative real-time PCR experiments (MIQE) were followed. The samples, their relevant controls, and inter-plate calibrators were organized in triplicates. Quant studio 1, 96 well plate detection system (Thermofisher Scientific, Massachusetts, USA) was set up to run quantitative PCR expression of BAX, Bcl_2, claudin-5, Caspase-3, INSR, IRS-1, and occludin in the cDNA samples. Each 12 μl PCR well contained 1.52 μl of RNAase- free water, 6 μl Power Up SYBER Green Master Mix (Applied Biosystems; A25742; Austin, Texas, USA), 0.24 Forward and Reverse Primer, and 4 μl diluted cDNA samples. Thermocycler conditions were set for a reaction volume of 12 μl, the hold step was set at 50 °C for 2 min, 95 °C for 2 min (X40 cycles), the PCR step was set at 95 °C for 15 s, 60 °C for 1 min, 72 °C for 1 min, and melt curve step was sat at 95 °C for 15 s, 95 °C for 15 s, 60 °C for 1 min and 95 °C for 15 s. Two housekeeping genes (β actin and GAPDH) were used to control for error and all primers were procured from Inquaba Biotechnical industries (Hatfield, Pretoria, South Africa). Samples were quantified by a standard curve and the calculation of the expression fold for each gene of interest was by the ΔΔ CT method. The primer pair sequence for each gene of interest and housekeeping gene was designed on the IDT website and verified using the Oligoanalyser tool (Table 1).

2.5. Enzyme-linked immunoassay of proinflammatory cytokines (IL-1α, IL-6, TNFα) and oxidative stress markers (GPX, and MDA)

Dissected brain samples from each hemisphere per animal were homogenized and used were used to run an enzyme-linked immunosorbent assay for proinflammatory cytokines (Rat IL-1α, Rat IL-6, Rat TNFα) according to the manufacturer's protocol (Elabscience, USA; E-EL-R0011, E-EL-R0015, E-EL-R0019 respectively). Oxidative stress markers were assessed using a malondialdehyde (MDA) Colorimetric assay kit: TBA method (Elabscience, Houston, Texas USA; E-BC-K025-M), and Glutathione Peroxidase (GSH-Px) Activity Assay Kit (Elabscience, Houston, Texas USA; E-BC-K096-M WST-1 Method). All samples were diluted 1:2, all standards, and run-in duplicates. The optical density (OD) values were read at 450 nm. The analysis for MDA was according to the TBA colorimetric method following the manufacturer's protocol, the concentration was calculated in μmol/g protein. The OD was read at 620 nm using an Anthos 2010, 96 well plate reader coupled to an ADAP software. OriginPro software was used to calculate the concentration of cytokines in the samples from obtained OD values according to the manufacturer's directions in pg/ml. The total protein concentration for each sample of brain homogenate was tested using Bradford reagent., The standards were made up in bovine serum albumin (BSA), and the calculated concentration of protein in each sample was applied in calculating the final concentration of cytokines (pg/mg of protein).

Table 1
Primer sequence for the gene of interest and housekeeping genes.

Gene	Primer pairs
BAX	Fwd: 5′GGTGAACTGGGGGAGGATTG3′ Rev: 5′AGAGCGATGTTGTCCACCAG3′
Bcl_2	Fwd: 5′GGTGAACTGGGGGAGGATTG3′ Rev: 5′AGAGCGATGTTGTCCACCAG3′
Caspase-3	Fwd: 5′GGAGCTTGGAACGCGAAGA3′ Rev: 5′ACACAAGCCCATTTCAGGGT3′
Claudin-5	Fwd: 5′CGAGGCAAGTTAGGTTGGGT3′ Rev: 5′GGTCGGTCAAGTCCTCACAA3′
Occludin	Fwd: 5′TTCTGTGCTCACAGGTGGTT3′ Rev: 5′TGGGCTGGATGCCAATTTAGT3′
INSR	Fwd: 5′TGTGACTGATTATTTAGATGTCCCA3′ Rev: 5′CATCTGGCTGCCTCTTCCTC3′
IRS-1	Fwd: 5′CTGCATAATCGGGCAAAGGC' Rev: 5′GCCCGTGTCATAGCTCAAGT3′
GAPDH Housekeeping	Fwd: 5′AAGAAGGTGGTGAAGCA GG3′ Rev:5′CAAAGGTGGAAGAATGG GAG3′
ACTB Housekeeping	Fwd: 5′AACCTTCTTGCAGCTCCTC3′ Rev: 5′ACCCATACCCACCATCAC AC3′

2.6. Histomorphometry using Giemsa stain and immunohistochemistry for neurogenesis

Each brain hemisphere per animal (in each treatment group) was placed in sucrose overnight and mounted on a freezing microtome with dry ice and sucrose and cut in the sagittal plane at 50 μm. Six brain sections were serially collected (36 sections per group) at 300 μm apart, between Bregma plate 169 to plate 177 corresponding to the rat brain atlas [52]. The first series of sections were stained with Giemsa solution (Sigma-Aldrich, Product number 1.09204.00) made up in potassium dihydrogen phosphate (pH 4.5) for neuronal histomorphology, while the next two series of sections were used for immunohistochemical labelling of Ki67 and DCX, respectively.

2.6.1. Neuronal number and nuclei area

Within each Giemsa-stained section, nine camera fields were captured at X1000 magnification from uniformly selected areas of the hippocampal regions. Two camera fields each were captured within the CA1 and CA3 regions respectively while five camera fields were captured from the dentate gyrus (DG) region; two from each arm and one from the apex of the dentate gyrus giving a total of three hundred and twenty-four camera fields per group that was analysed. The number of neurons and nuclei area in the upper focal plane of these camera fields were determined using the cell counter and trace plugins of ImageJ software respectively. Only neurons with a vesicular nucleus and centrally placed nucleoli were measured and counted. Representative photomicrographs were compiled using Microsoft Visio and no manipulation was made to the captured images except for brightness and contrast.

2.6.2. Volume of the dentate gyrus

Photomicrographs of the Giemsa-stained dorsal hippocampus of each brain section was obtained using a Leica ICC50 HD video camera linked to a Leica DM 500 microscope (Leica Biosystems, USA). Within each section, the entire dorsal hippocampus was captured at X25 magnification, all 6 camera fields per group were imported in a stacked sequence, and the image j Volumest plugin was used in quantifying the volume of the granular layer and molecular layer in the dentate gyrus of each animal per group. The Volumest plugin entails a combination of the grid and Cavalieri's principle obtained by tracing out the region of interest for each of these layers in each camera field of an image sequence and the estimated volume for each layer was obtained in mm^3.

2.6.3. Immunohistochemistry for neurogenesis

From each brain hemisphere, six sections between plates 172–177 were selected using the atlas of the rat brain [52] for each histochemical

labelling. Free-floating brain sections in 24 well plates first underwent endogenous peroxidase inhibition with 50% methanol, 50% PB, and 1.66% hydrogen peroxide. Sections were washed, then blocked in 3% normal goat serum, 2% (BSA), and 0.25% Triton x 100 in 0.1 M PB for 2hrs at room temperature, followed by incubation in the primary antibodies (rabbit polyclonal antibody; Abcam, Cambridge, MA, USA), Ki67 and DCX (Abcam, USA; AB15580 and AB18723 respectively) with dilution factors 1:1000 and 1:3000 respectively for 48 hrs. The sections were washed with 0.1PB and incubated for 2 hr with secondary antibody (goat anti-rabbit antibody IgGs; Vectastain, Burlingame, CA USA). Washed and incubated for 1 hr with ABC kit (Vectastain, Burlingame, CA USA) and stained with DAB, mounted on gelatine-coated slides, dehydrated, and cleared in xylene. Control sections were incubated in 0.1MPB omitting the primary antibody. Photomicrographs of Ki67 and DCX immunolocalized dorsal hippocampus brain sections were obtained and counts of immunolabelled cells were determined by the cell counter plugin of Image J. Only DCX cells in the upper focal plane with a pale centrally placed centre were counted while immunolocalized cells for Ki67 were counted in clusters.

2.7. Statistical analysis

The diabetic parameters, number, and nuclei area of neurons in hippocampal regions, concentrations of cytokines and oxidative markers, expression of hippocampal Ki67 and DCX labelling as well as gene expression mRNA levels of insulin receptors, junctional and apoptotic genes were recorded as mean ± SEM. The data were subjected to a normality test using the Shapiro-Wilks test, parametric data were analysed using a one-way ANOVA test and a Post hoc Bonferroni's test was conducted to determine the difference between the groups. Nonparametric data were analysed by the Kruskal Wallis test and a Post hoc Duncan's pairwise analysis. The results with $P < 0.05$ were regarded as significant. All data analysis was carried out using the IBM SPSS statistics version 28.

2.8. Ethical clearance

This study was approved by the Animal Research Ethics Committee (approval number 2018/011/58/C) of the University of the Witwatersrand. All experimental animal handling and treatments were carried out according to the standards and principles set forth by this committee.

3. Results

3.1. Food, fluid consumption, and blood glucose across experimental groups

A decrease in food intake across treated groups was observed with a significant reduction in AL, AA, DAL, and DAA compared to the control (Fig. 1A). The diabetic groups consumed more fluid compared to the other groups with a significant increase in water consumption in DB and

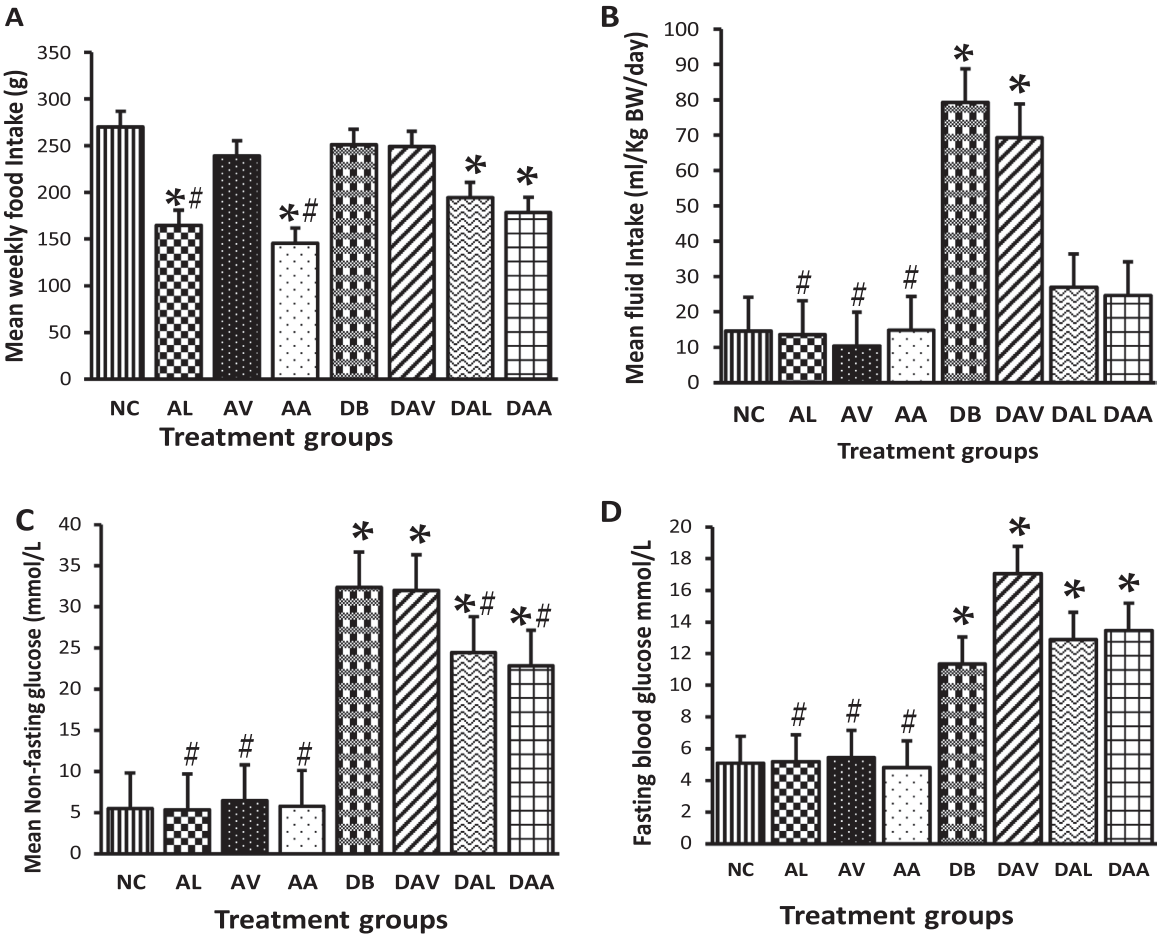

Fig. 1. Mean food and fluid intake, non-fasting, and fasting blood glucose across groups. A) Significant difference in mean food intake between groups (One way ANOVA $P = 0.001$). B) Significant difference in mean fluid intake between groups (Kruskal Wallis test, $P = 0.001$). C, D) Significant difference in mean random NFBG and FBG (One way ANOVA $P > 0.001$). $n = 6$ '*' significantly different compared to control, '#' significantly different compared to diabetes $P \leq 0.05$. NC: Control, AV: cART, AL: alcohol, AA: cART and alcohol, DB: diabetic, DAV: diabetic and cART, DAL: diabetic and alcohol, DAA diabetic cART and alcohol.

3.4. Proinflammatory cytokines and oxidative stress markers

The mean concentrations of proinflammatory cytokines across all the experimental groups are reported in Table 2. The concentration of IL-6 is significantly elevated in the AL, AV, and DAA groups compared to the control and AA groups. The concentration level of TNFα is significantly elevated in AL and AV groups compared to the control. While the concentration level of IL-1α is significantly elevated in the AL and DAA groups compared to the control and AA groups. Furthermore, the concentration of IL-1α, IL-6, and TNFα in DB and DAV groups reduced significantly against the control and all other treated groups but no significant difference occurs between cytokine levels in DB and DAV groups (Table 2). The lipid peroxidation levels recorded are significantly increased in all the experimental groups (AL, AV, DB, DAV, DAL, and DAA) in comparison to the control except for the AA group. However, MDA levels in the AL and DAV group were significantly increased compared to the AA group. Also, the antioxidant (GP_X) level was significantly reduced in all the experimental groups (AL, AV, AA, DB, DAV, DAL, and DAA) relative to the control and significantly reduced in the AA, DB, DAV, and DAL groups compared to AL and DAA groups (Table 2).

3.5. Mean expression of membrane-associated junctional proteins in the hippocampal tissue

The analysis of claudin-5 and occludin expression levels in the hippocampus reveals mostly the downregulation of these junctional proteins across the experimental groups (Fig. 3 A-B). Claudin-5 was observed to be significantly downregulated in the AA, AV, DB, and DAV groups compared to the control (P = 0.031, 0.004, 0.034, and 0.043) but downregulated in the AV group compared to the AL, DB, DAV, DAL, and DAA groups (P = 0.004, 0.015, 0.007, 0.001, 0.027; Fig. 3A). Occludin was significantly downregulated in the DAA group compared to the control (P = 0.045) and also downregulated in the AA and DB groups compared to the control (P = 0.023, 0.017), AV (P = 0.003, 0.001) and DAL groups (P = 0.025 and 0.002; Fig. 3 B).

3.6. Mean fold expression of apoptotic genes in hippocampal tissue

The mRNA expression of the three major apoptotic markers is shown in Fig. 3 with significant up up-regulation of Bcl_2 in the DAL, and DAA groups compared to the control (P = 0.045, and 0.029 respectively), and compared to the DB (P = 0.001) and DAV groups (P = 0.018 and 0.015). Conversely, Bcl_2 mRNA expression in the AA group is downregulated compared to control, AL, AV, DAL, and DAA (P = 0.03, 0.039, 0.023, 0.015, and 0.001 respectively, Fig. 4A). For BAX, a significant up-regulation was observed in the DAL compared to the control, AL, and DB groups (P = 0.001) and upregulated in the AL, DB, DAV, and DAA groups compared to the control (P = 0.01) and AV groups (P = 0.001). Similarly, BAX mRNA expression in the AA group is downregulated compared to control, AL, AV, DB, DAV, DAL, and DAA (P = 0.032, 0.014, 0.05, 0.031, 0.048, 0.001, 0.04 respectively, Fig. 4B). Caspase-3 in DB, DAV, DAL, and DAA was significantly upregulated against the control (P = 0.037, 0.001, 0.020, and 0.036) and AA (P = 0.032, 0.001, 0.017, and 0.031); and significantly upregulated in DAV compared to AL and AV treated groups (P = 0.009 and 0.003, Fig. 4C). The ratio of BAX to Bcl_2 reveal increased fold expression of BAX mRNA compared to Bcl_2 in the AL, DB, DAV, DAL and DAA, a reduced ratio in the AV and uniform levels in the AA group (Fig. 4D).

3.7. Mean number of neurons in different hippocampal regions

The estimated number of neurons in different hippocampal regions was significantly reduced, mostly in the diabetic groups (DB, DAV, DAL, and DAA) compared to other groups (Figs. 5–7). In the CA1 region, a uniform row of principal cells (circle, Fig. 5) and few peripheral glial cells (black arrows, Fig. 5) are seen in the NC group, followed closely by the AA, and AV groups. The CA1 neuronal number (CA1N) in the DAV, DAL, and DAA are significantly reduced compared to control, AL, AV, AA, and DB (P = 0.001). AL and DB are significantly decreased compared to control (P = 0.007 and 0.004; Fig. 5A) with a thin row of neurons, of which some present pyknotic nuclei (red arrows, Fig. 5) observed especially in the DAA group. In the CA3 region, a cluster of uniformly sized cell neurons with few glial cell nuclei are observed in the control group, and slightly similar histology was observed in the AA, and AV groups (Fig. 6). There number of neurons in the CA3 (CA3N) is significantly reduced in the DAV and DAL are significantly reduced compared to control (P = 0.001), AV (P = 0.016 and 0.005) and AA (P = 0.001), while DAA is significantly reduced compared to control, AL, AV, AA, and DB (P = 0.001, 0.013, 0.001, 0.001 and 0.019; Fig. 6A, P < 0.05). Additionally, the neurons in the diabetic comorbidity groups (DAV, DAL, and DAA) appeared dispersed and diffused with few cells pyknotic (red arrows, Fig. 6). In the DG region, a wide and dense layer of granular cell neurons are observed in the control group (Fig. 7) with a significant reduction in neuronal number in all the experimental groups compared to the control (P < 0.05, Fig. 7A). The AL, AV, AA, DB, and DAA are significantly reduced compared to control (P = 0.001). DAL is significantly decreased compared to control and AV (P = 0.001 and 0.003). The DAV group is the most severely affected with significantly reduced DG neuronal number relative to the control, AL, AV, AA, and DAA groups (P = 0.001, 0.033, 0.001, 0.004, and 0.044 respectively; Fig. 8A), followed by the DAL with fewer granular neurons (Fig. 7).

3.8. Mean neuronal nuclei in different hippocampal regions

The neuronal nuclei area at all hippocampal regions (CA1, CA3, and DG) are significantly increased in the DB group compared to the control (NC), AV, DAV, DAL, and DAA groups (P = 0.05, Fig. 5 A,6 A, and 7 A),

Table 2
Mean concentration of cytokines IL-1α, IL-6, TNFα, and oxidative stress markers MDA and GPx in hippocampal tissue homogenate.

	IL-6 (pg/ mg protein)		TNF-α (pg/ mg protein)		IL-1α (pg/ mg protein)		GPx (pg/ mg protein)		MDA (μmol/g protein)	
	Mean	Std Err	Mean	Std Err	Mean	Std Err	Mean	Std Err	Mean	Std Err
NC	1.507	0.02	1.187	0.05	3.349	0.09	2.165	0.08	0.032	0.001
AL	1.888	0.10*#	1.429	0.04*#	3.982	0.2*#	1.505	0.09*#	0.077	0.002*
AV	1.840	0.05*#	1.333	0.03*#	3.774	0.15*#	1.278	0.01*	0.069	0.002*
AA	1.517	0.05#	1.098	0.03#	3.132	0.22#	1.186	0.01*	0.044	0.002
DB	1.104	0.01*	0.826	0.03*	2.455	0.01*	1.193	0.05*	0.065	0.006*
DAV	0.981	0.07*	0.847	0.01*	2.527	0.22*	1.187	0.04*	0.083	0.011*
DAL	1.780	0.11#	1.260	0.12#	3.908	0.13#	1.116	0.01*	0.066	0.004*
DAA	2.008	0.09*#	1.272	0.01#	4.035	0.12*#	1.476	0.10*#	0.061	0.002*

Data reported as mean ± SEM. Significant difference in the mean concentration of cytokines (IL-1α, IL-6, TNFα), MDA, and GPX between groups (One way ANOVA P = 0.001). '*' is significantly different compared to the control, and '#' is significantly different compared to diabetes P ≤ 0.05. n = 4. Key: NC: Control, AV: cART, AL: alcohol, AA: cART and alcohol, DB: diabetic, DAV: diabetic and cART, DAL: diabetic and alcohol, DAA diabetic cART and alcohol.

CRediT authorship contribution statement

Jaclyn Asouzu Johnson: Conceptualization, Methodology, Software, Data curation, Writing – original draft, Visualization, Investigation, Software, Validation, Writing – review & editing. **Rober Ndou**: Conceptualization, Resources, Supervision. **Ejikeme F Mbajiorgu**: Conceptualization, Methodology, Data curation, Writing – original draft preparation, Supervision, Validation, Writing – review & editing.

Declaration of Competing Interest

The authors declare that they have no known competing financial interests or personal relationships that could have appeared to influence the work reported in this paper.

Data Availability

Data will be made available on request.

Acknowledgments

Our appreciation goes to our co-workers, Eguavoen Idemudia and Vaughan Perry for their excellent collaborative efforts. And special appreciation goes to Mrs. Hasiena Ali for her technical and laboratory assistance.

Institutional review board statement

The study was conducted in accordance with the standards and principles set forth by the Wits Research Animal Facility (WRAF) (approval number 2018/011/58/C) of the University of the Witwatersrand.

References

[1] D. Accili, Can COVID-19 cause diabetes? Nat. Metab. 3 (2021) 123–125 (Available at), ⟨https://www.nature.com/articles/s42255-020-00339-7⟩.
[2] A.T. Ahmed, A.J. Karter, E.M. Warton, J.U. Doan, C.M. Weisner, The relationship between alcohol consumption and glycemic control among patients with diabetes: the kaiser permanente northern california diabetes registry, J. Gen. Intern. Med. 23 (2008) 275–282 (Available at), ⟨https://www.ncbi.nlm.nih.gov/pmc/articles/PMC2359478/⟩.
[3] C. Akay, et al., Antiretroviral drugs induce oxidative stress and neuronal damage in the central nervous system, J. Neurovirol. 20 (2014) 39–53.
[4] S.E. Arnold, Z. Arvanitakis, S.L. Macauley-Rambach, A.M. Koenig, H.-Y. Wang, R. S. Ahima, S. Craft, S. Gandy, C. Buettner, L.E. Stoeckel, D.M. Holtzman, D. M. Nathan, Brain insulin resistance in type 2 diabetes and Alzheimer disease: concepts and conundrums, Nat. Rev. Neurol. 14 (2018) 168–181.
[5] J. Asouzu Johnson, R. Ndou, E.F. Mbajiorgu, Combination Antiretroviral Therapy (cART) in diabetes exacerbates diabetogenic effects on hippocampal microstructure, neurogenesis and cytokine perturbation in male Sprague Dawley rats, Diagn. (2022). ⟨https://www.ncbi.nlm.nih.gov/pmc/articles/PMC9029837/⟩.
[6] A.D. Association, 2. Classification and diagnosis of diabetes, Diabetes Care 38 (2015) S8–S16.
[7] L. Bertrand, L. Dygert, M. Toborek, Antiretroviral treatment with efavirenz disrupts the blood-brain barrier integrity and increases stroke severity, Sci. Rep. 6 (2016) 39738.
[8] G.J. Biessels, F. Despa, Cognitive decline and dementia in diabetes: mechanisms and clinical implications, Nat. Rev. Endocrinol. 14 (2018) 591–604. ⟨https://www.ncbi.nlm.nih.gov/pmc/articles/PMC6397437/⟩.
[9] G.J. Biessels, L.P. Reagan, Hippocampal insulin resistance and cognitive dysfunction, Nat. Rev. Neurosci. 16 (2015) 660–671.
[10] A. Borsini, M.G. Di Benedetto, J. Giacobbe, C.M. Pariante, Pro- and Anti-Inflammatory properties of interleukin in vitro: relevance for major depression and human hippocampal neurogenesis, Int. J. Neuropsychopharmacol. 23 (2020) 738–750, https://doi.org/10.1093/ijnp/pyaa055. Accessed May 10, 2022.
[11] K.M. Broadhouse, L. Mowszowski, S. Duffy, I. Leung, N. Cross, M.J. Valenzuela, S. L. Naismith, Memory performance correlates of hippocampal subfield volume in mild cognitive impairment subtype, Front. Behav. Neurosci. (2019) 13. ⟨https://www.frontiersin.org/articles/10.3389/fnbeh.2019.00259⟩ [Accessed January 4, 2023].
[12] T.T. Brown, S.R. Cole, X. Li, L.A. Kingsley, F.J. Palella, S.A. Riddler, B.R. Visscher, J.B. Margolick, A.S. Dobs, Antiretroviral therapy and the prevalence and incidence of diabetes mellitus in the multicenter AIDS cohort study, Arch. Intern. Med. 165 (2005) 1179–1184.
[13] R.B. Camire, H.J. Beaulac, C.L. Willis, Transitory loss of glia and the subsequent modulation in inflammatory cytokines/chemokines regulate paracellular claudin-5 expression in endothelial cells, J. Neuroimmunol. 284 (2015) 57–66.
[14] S. Carlsson, N. Hammar, V. Grill, J. Kaprio, Alcohol consumption and the incidence of type 2 diabetes: a 20-year follow-up of the Finnish twin cohort study, Diabetes Care 26 (2003) 2785–2790.
[15] E. Cherubini, R. Miles, The CA3 region of the hippocampus: how is it? What is it for? How does it do it? Front. Cell Neurosci. 9 (2015) 19. ⟨https://www.ncbi.nlm.nih.gov/pmc/articles/PMC4318343/⟩.
[16] A. Chodobski, B.J. Zink, J. Szmydynger-Chodobska, Blood-brain barrier pathophysiology in traumatic brain injury, Transl. Stroke Res. 2 (2011) 492–516 (Available at), ⟨https://www.ncbi.nlm.nih.gov/pmc/articles/PMC3268209/⟩.
[17] M. Cyuńczyk, M.E. Zujko, J. Jamiołkowski, K. Zujko, M. Łapińska, M. Zalewska, M. Kondraciuk, A.M. Witkowska, K.A. Kamiński, Dietary total antioxidant capacity is inversely associated with prediabetes and insulin resistance in bialystok PLUS population, Antioxidants 11 (2022) 283.
[18] J. Czerniawski, T. Miyashita, G. Lewandowski, J.F. Guzowski, Systemic lipopolysaccharide administration impairs retrieval of context–object discrimination, but not spatial, memory: Evidence for selective disruption of specific hippocampus-dependent memory functions during acute neuroinflammation, Brain Behav. Immun. 44 (2015) 159–166. ⟨https://www.sciencedirect.com/science/article/pii/S088915911400467X⟩.
[19] R. Daneman, A. Prat, The blood–brain barrier, Cold Spring Harb. Perspect. Biol. 7 (2015) a020412.
[20] De Felice F.G., Ferreira S.T., 2014. Inflammation, Defective Insulin Signaling, and Mitochondrial Dysfunction as Common Molecular Denominators Connecting Type 2 Diabetes to Alzheimer Disease. Diabetes 63:2262–2272 Available at: https://doi.org/10.2337/db13–1954 [Accessed September 20, 2022].
[21] De Meyts P., 2000. The Insulin Receptor and Its Signal Transduction Network. In: Endotext (Feingold KR et al., eds). South Dartmouth (MA): MDText.com, Inc. Available at: http://www.ncbi.nlm.nih.gov/books/NBK378978/ [Accessed June 30, 2022].
[22] E.J. Donzis, N.C. Tronson, Modulation of learning and memory by cytokines: Signaling mechanisms and long term consequences, Neurobiol. Learn. Mem. 115 (2014) 68–77 (Available at), ⟨https://www.sciencedirect.com/science/article/pii/S1074742714001543⟩.
[23] L. Doos, E.O. Roberts, N. Corp, U.T. Kadam, Multi-drug therapy in chronic condition multimorbidity: a systematic review, Fam. Pr. 31 (2014) 654–663 (Available at), ⟨https://www.ncbi.nlm.nih.gov/pmc/articles/PMC5942538/⟩.
[24] S. Elmore, Apoptosis: a review of programmed cell death, Toxicol. Pathol. 35 (2007) 495–516. ⟨https://www.ncbi.nlm.nih.gov/pmc/articles/PMC2117903/⟩.
[25] P.A. Engler, S.E. Ramsey, R.J. Smith, Alcohol use of diabetes patients: The need for assessment and intervention, Acta Diabetol. 50 (2013) 93–99 (Available at), ⟨https://www.ncbi.nlm.nih.gov/pmc/articles/PMC2954251/⟩.
[26] S. Ferlita, A. Yegiazaryan, N. Noori, G. Lal, T. Nguyen, K. To, V. Venketaraman, Type 2 diabetes mellitus and altered immune system leading to susceptibility to pathogens, especially mycobacterium tuberculosis, J. Clin. Med. 8 (2019) 2219. ⟨https://www.ncbi.nlm.nih.gov/pmc/articles/PMC6947370/⟩.
[27] S.L. Fink, B.T. Cookson, Apoptosis, pyroptosis, and necrosis: mechanistic description of dead and dying eukaryotic cells, Infect. Immun. 73 (2005) 1907–1916. ⟨https://www.ncbi.nlm.nih.gov/pmc/articles/PMC1087413/⟩.
[28] C. Gabay, Interleukin-6 and chronic inflammation, Arthritis Res. Ther. 8 (2006) S3, https://doi.org/10.1186/ar1917. Accessed May 10, 2022.
[29] U. Galicia-Garcia, A. Benito-Vicente, S. Jebari, A. Larrea-Sebal, H. Siddiqi, K. B. Uribe, H. Ostolaza, C. Martín, Pathophysiology of type 2 diabetes mellitus, Int. J. Mol. Sci. 21 (2020) 6275 (Available at), ⟨https://www.ncbi.nlm.nih.gov/pmc/articles/PMC7503727/⟩.
[30] B. Guthrie, B. Makubate, V. Hernandez-Santiago, T. Dreischulte, The rising tide of polypharmacy and drug-drug interactions: population database analysis 1995–2010, BMC Med. 13 (2015) 74, https://doi.org/10.1186/s12916-015-0322-7. Accessed July 16, 2022.
[31] J. Haorah, S.H. Ramirez, N. Floreani, S. Gorantla, B. Morsey, Y. Persidsky, Mechanism of alcohol-induced oxidative stress and neuronal injury, Free Radic. Biol. Med 45 (2008) 1542–1550 (Available at), ⟨https://www.ncbi.nlm.nih.gov/pmc/articles/PMC2605399/⟩.
[32] G.J. Harry, A.D. Kraft, Neuroinflammation and microglia: considerations and approaches for neurotoxicity assessment, Expert Opin. Drug Metab. Toxicol. 4 (2008) 1265–1277 (Available at), ⟨https://www.ncbi.nlm.nih.gov/pmc/articles/PMC2658618/⟩.
[33] N. Ho, M.S. Sommers, I. Lucki, Effects of diabetes on hippocampal neurogenesis: links to cognition and depression, Neurosci. Biobehav. Rev. 37 (2013) 1346–1362. ⟨https://www.ncbi.nlm.nih.gov/pmc/articles/PMC3788092/⟩.
[34] C.-C. Huang, C.-C. Lee, K.-S. Hsu, The role of insulin receptor signaling in synaptic plasticity and cognitive function, Chang Gung Med. J. 33 (2010) 115–125.
[35] B. Hussain, C. Fang, J. Chang, Blood–brain barrier breakdown: an emerging biomarker of cognitive impairment in normal aging and dementia, Front. Neurosci. (2021) 15. ⟨https://www.frontiersin.org/articles/10.3389/fnins.2021.688090⟩.
[36] K. Iglay, H. Hannachi, P. Joseph Howie, J. Xu, X. Li, S.S. Engel, L.M. Moore, S. Rajpathak, Prevalence and co-prevalence of comorbidities among patients with type 2 diabetes mellitus, Curr. Med. Res. Opin. 32 (2016) 1243–1252.
[37] Ishunina T.A., Bogolepova I.N., Swaab D.F., 2019. Increased Neuronal Nuclear and Perikaryal Size in the Medial Mamillary Nucleus of Vascular Dementia and Alzheimer's Disease Patients: Relation to Nuclear Estrogen Receptor α. DEM 47: 274–280 Available at: https://www.karger.com/Article/FullText/500244 [Accessed July 3, 2021].

[38] H.B. Jang, M.J. Go, S.I. Park, H.-J. Lee, S.B. Cho, Chronic heavy alcohol consumption influences the association between genetic variants of GCK or INSR and the development of diabetes in men: a 12-year follow-up study, Sci. Rep. 9 (2019) 20029. ⟨https://www.nature.com/articles/s41598-019-56011-y⟩.

[39] U. Kadam, I. Roberts, S. White, R. Bednall, K. Khunti, P. Nilsson, C. Lawson, Conceptualising multiple drug use in patients with comorbidity and multimorbidity: proposal for standard definitions beyond the term polypharmacy, J. Clin. Epidemiol. (2018) 106.

[40] S.-J. Kim, D.-J. Kim, Alcoholism and diabetes mellitus, Diabetes Metab. J. 36 (2012) 108–115.

[41] A. Kołota, D. Głąbska, M. Oczkowski, J. Gromadzka-Ostrowska, Influence of alcohol consumption on body mass gain and liver antioxidant defense in adolescent growing male rats, Int. J. Environ. Res. Public Health (2019) 16 (Available at), ⟨https://www.ncbi.nlm.nih.gov/pmc/articles/PMC6651161/⟩.

[42] S. Kumar, M. Jin, A. Ande, N. Sinha, P.S. Silverstein, A. Kumar, Alcohol consumption effect on antiretroviral therapy and HIV-1 pathogenesis: role of cytochrome P450 isozymes, Expert Opin. Drug Metab. Toxicol. 8 (2012) 1363–1375 (Available at), ⟨https://www.ncbi.nlm.nih.gov/pmc/articles/PMC4033313/⟩.

[43] J.X. Liu, S.B. Pinnock, J. Herbert, Novel control by the CA3 region of the hippocampus on neurogenesis in the dentate gyrus of the adult rat, PLoS One 6 (2011), e17562.

[44] Q. Ma, F. Vaida, J. Wong, C.A. Sanders, Y. Kao, D. Croteau, D.B. Clifford, A. C. Collier, B.B. Gelman, C.M. Marra, J.C. McArthur, S. Morgello, D.M. Simpson, R. K. Heaton, I. Grant, S.L. Letendre, CHARTER Group, Long-term efavirenz use is associated with worse neurocognitive functioning in HIV-infected patients, J. Neurovirol 22 (2016) 170–178.

[45] Masuku , 2019. HIV and antiretroviral therapy-induced metabolic syndrome in people living with HIV and its implications for care: A critical review. Available at: ⟨https://www.journalofdiabetology.org/article.asp?issn=2078–7685;year=2019;volume=10;issue=2;spage=41;epage=47;aulast=Masuku⟩ [Accessed May 17, 2021].

[46] S.A. Meda, K.A. Hawkins, A.D. Dager, H. Tennen, S. Khadka, C.S. Austad, R. M. Wood, S. Raskin, C.R. Fallahi, G.D. Pearlson, Longitudinal effects of alcohol consumption on the hippocampus and parahippocampus in college students, Biol. Psychiatry Cogn. Neurosci. Neuroimaging 3 (2018) 610–617 (Available at), ⟨https://www.ncbi.nlm.nih.gov/pmc/articles/PMC6062479/⟩.

[47] N.T. Milne, R.S. Bucks, W.A. Davis, T.M.E. Davis, R. Pierson, S.E. Starkstein, D. G. Bruce, Hippocampal atrophy, asymmetry, and cognition in type 2 diabetes mellitus, Brain Behav. 8 (2017), e00741 (Available at), ⟨https://www.ncbi.nlm.nih.gov/pmc/articles/PMC5853633/⟩.

[48] S.A. Morris, D.W. Eaves, A.R. Smith, K. Nixon, Alcohol inhibition of neurogenesis: a mechanism of hippocampal neurodegeneration in an adolescent alcohol abuse model, Hippocampus 20 (2010) 596–607.

[49] H. Nagano, S. Ito, T. Masuda, S. Ohtsuki, Effect of insulin receptor-knockdown on the expression levels of blood–brain barrier functional proteins in human brain microvascular endothelial cells, Pharm. Res. (2021), https://doi.org/10.1007/s11095-021-03131-8. Accessed June 28, 2022.

[50] S. Ohtsuki, H. Yamaguchi, Y. Katsukura, T. Asashima, T. Terasaki, mRNA expression levels of tight junction protein genes in mouse brain capillary endothelial cells highly purified by magnetic cell sorting, J. Neurochem 104 (2008) 147–154.

[51] F.N. Osuji, C.C. Onyenekwe, J.E. Ahaneku, N.R. Ukibe, The effects of highly active antiretroviral therapy on the serum levels of pro-inflammatory and anti-inflammatory cytokines in HIV infected subjects, J. Biomed. Sci. 25 (2018) 88, https://doi.org/10.1186/s12929-018-0490-9. Accessed August 20, 2021.

[52] G. Paxinos, C. Watson, The Rat Brain in Stereotaxic Coordinates: Hard Cover Edition, Elsevier, 2006.

[53] J. Pearson-Leary, E.C. McNay, Novel roles for the insulin-regulated glucose transporter-4 in hippocampally dependent memory, J. Neurosci. 36 (2016) 11851–11864.

[54] L. Qin, J. He, R.N. Hanes, O. Pluzarev, J.-S. Hong, F.T. Crews, Increased systemic and brain cytokine production and neuroinflammation by endotoxin following ethanol treatment, J. Neuroinflamm. 5 (2008) 10.

[55] J.L. Rains, S.K. Jain, Oxidative stress, insulin signaling and diabetes, Free Radic. Biol. Med. 50 (2011) 567–575. ⟨https://www.ncbi.nlm.nih.gov/pmc/articles/PMC3557825/⟩.

[56] L.P. Reagan, H.B. Cowan, J.L. Woodruff, G.G. Piroli, J.M. Erichsen, A.N. Evans, H. E. Burzynski, N.D. Maxwell, F.Z. Loyo-Rosado, V.A. Macht, C.A. Grillo, Hippocampal-specific insulin resistance elicits behavioral despair and hippocampal dendritic atrophy, Neurobiol. Stress 15 (2021), 100354. ⟨https://www.sciencedirect.com/science/article/pii/S235228952100062X⟩.

[57] K. Rehman, M.S.H. Akash, A. Liaqat, S. Kamal, M.I. Qadir, A. Rasul, Role of Interleukin-6 in development of insulin resistance and type 2 diabetes mellitus, Crit. Rev. Eukaryot. Gene Expr. 27 (2017) 229–236.

[58] C. Reinke, N. Buchmann, A. Fink, C. Tegeler, I. Demuth, G. Doblhammer, Diabetes duration and the risk of dementia: a cohort study based on German health claims data, Age Ageing 51 (2022) afab231, https://doi.org/10.1093/ageing/afab231. Accessed April 22, 2022.

[59] P. Rheeder, Type 2 diabetes: the emerging epidemic. South African, Fam. Pract. 48 (2006), 20–20.

[60] C. Richard, M. Wadowski, S. Goruk, L. Cameron, A.M. Sharma, C.J. Field, Individuals with obesity and type 2 diabetes have additional immune dysfunction compared with obese individuals who are metabolically healthy, BMJ Open Dia.b Res. Care 5 (2017), e000379 (Available at), ⟨https://drc.bmj.com/lookup/doi/10.1136/bmjdrc-2016-000379⟩.

[61] T.S. Salameh, W.G. Mortell, A.F. Logsdon, D.A. Butterfield, W.A. Banks, Disruption of the hippocampal and hypothalamic blood–brain barrier in a diet-induced obese model of type II diabetes: prevention and treatment by the mitochondrial carbonic anhydrase inhibitor, topiramate, Fluids Barriers CNS 16 (2019) 1, https://doi.org/10.1186/s12987-018-0121-6. Accessed May 9, 2022.

[62] J. Shi, J. Fan, Q. Su, Z. Yang, Cytokines and abnormal glucose and lipid metabolism, Front. Endocrinol. (2019) 10. ⟨https://www.frontiersin.org/articles/10.3389/fendo.2019.00703/full⟩.

[63] A.S. Smith, S. Ankam, R.C.B. Basa, K.L. Gordon, A.V. Terskikh, K.L. Jordan-Sciutto, J. Price, P.M. McDonough, HIV antiretrovirals have differential effects on viability and function in human iPSC-derived neurons and neural precursor cells, bioRxiv (2020), 2020.09.05.284422 Available at, ⟨https://www.biorxiv.org/content/10.1101/2020.09.05.284422v1⟩.

[64] M. Spinelli, S. Fusco, C. Grassi, Brain insulin resistance and hippocampal plasticity: mechanisms and biomarkers of cognitive decline, Front. Neurosci. 13 (2019). ⟨https://www.frontiersin.org/article/10.3389/fnins.2019.00788⟩.

[65] K.S. Tan, K.O. Lee, K.C. Low, A.M. Gamage, Y. Liu, G.-Y.G. Tan, H.Q.V. Koh, S. Alonso, Y.-H. Gan, Glutathione deficiency in type 2 diabetes impairs cytokine responses and control of intracellular bacteria, J. Clin. Investig. 122 (2012) 2289–2300. ⟨https://www.ncbi.nlm.nih.gov/pmc/articles/PMC3366396/⟩.

[66] P. Tien, M. Schneider, S. Cole, A. Levine, M. Cohen, J. Dehovitz, M. Young, J. Justman, Antiretroviral therapy exposure and insulin resistance in the Women's Interagency HIV study, J. Acquir. Immune Defic. Syndr. (1999) 49 (2008) 369–376.

[67] L.B. Tovar-y-Romo, N.N. Bumpus, D. Pomerantz, L.B. Avery, N. Sacktor, J. C. McArthur, N.J. Haughey, Dendritic spine injury induced by the 8-hydroxy metabolite of efavirenz, J. Pharmacol. Exp. Ther. 343 (2012) 696–703.

[68] A. Tseng, J. Seet, E.J. Phillips, The evolution of three decades of antiretroviral therapy: challenges, triumphs and the promise of the future, Br. J. Clin. Pharm. 79 (2015) 182–194 (Available at), ⟨https://www.ncbi.nlm.nih.gov/pmc/articles/PMC4309625/⟩.

[69] Y.-F. Tu, S.-T. Jiang, C.-W. Chiang, L.-C. Chen, C.-C. Huang, Endothelial-specific insulin receptor substrate-1 overexpression worsens neonatal hypoxic-ischemic brain injury via mTOR-mediated tight junction disassembly, Cell Death Discov. 7 (2021) 1–11. ⟨https://www.nature.com/articles/s41420-021-00548-3⟩.

[70] L.P. van der Heide, A. Kamal, A. Artola, W.H. Gispen, G.M.J. Ramakers, Insulin modulates hippocampal activity-dependent synaptic plasticity in a N-methyl-d-aspartate receptor and phosphatidyl-inositol-3-kinase-dependent manner, J. Neurochem. 94 (2005) 1158–1166.

[71] S.H. Vermund, E.K. Sheldon, M. Sidat, Southern Africa: the highest priority region for HIV prevention and care interventions, Curr. HIV/AIDS Rep. 12 (2015) 191–195.

[72] C.M.O. Volpe, P.H. Villar-Delfino, P.M.F. dos Anjos, J.A. Nogueira-Machado, Cellular death, reactive oxygen species (ROS) and diabetic complications, Cell Death Dis. 9 (2018) 1–9. ⟨https://www.nature.com/articles/s41419-017-0135-z⟩.

[73] D.R. Whiting, L. Guariguata, C. Weil, J. Shaw, IDF diabetes atlas: global estimates of the prevalence of diabetes for 2011 and 2030, Diabetes Res. Clin. Pract. 94 (3) (2011) 311–321. ⟨https://www.sciencedirect.com/science/article/pii/S0168822711005912⟩.

[74] R.D. Wilson, M.S. Islam, Fructose-fed streptozotocin-injected rat: an alternative model for type 2 diabetes, Pharmacol. Rep. 64 (2012) 129–139.

[75] W. Zhao, H. Chen, H. Xu, E. Moore, N. Meiri, M.J. Quon, D.L. Alkon, Brain insulin receptors and spatial memory. Correlated changes in gene expression, tyrosine phosphorylation, and signaling molecules in the hippocampus of water maze trained rats, J. Biol. Chem. 274 (1999) 34893–34902.

[76] U. Ziegler, P. Groscurth, Morphological features of cell death, N. Physiol. Sci. 19 (2004) 124–128.